RSC Advances

PAPER

View Article Online
View Journal | View Issue

Check for updates

Cite this: *RSC Adv.*, 2026, **16**, 5785

Valorization of ethylene carbonate recovered from spent lithium-ion battery electrolytes: synthesis and properties of biodegradable poly ethylene succinate-*co*-ethylene glycol (PESG) copolyesters

Huaze Liu,† Xiaolong Li,† Yuanyuan Zhao, Haiyue Wang * and Liying Guo *

This study proposes a green closed-loop strategy aimed at valorizing ethylene carbonate (EC), a high-boiling organic component found in spent lithium-ion battery (LIB) electrolytes, into degradable polyester materials. First, EC was recovered through vacuum distillation at 150 °C and 0.09 MPa, yielding the target product with an 86.5% yield and 96.9% purity. Subsequently, benchmark polyester polyethylene glycol succinate (PES) was synthesized from EC and dimethyl succinate (DMSu) *via* a polycondensation reaction catalyzed by dibutyltin oxide (Bu_2SnO). The resulting material exhibited a viscosity of 0.42 dL g^{-1}, a thermal weight loss of 5% at 315 °C, and a glass transition temperature (T_g) of −9.5 °C. To further enhance the flexibility and biodegradability of PES, short-chain diol ethylene glycol (EG) was introduced as a third monomer, and a one-pot random copolymerization reaction was conducted to prepare six PESG copolymers with EC : EG molar ratios ranging from 10 : 0 to 5 : 5. The esterification–polycondensation process conditions were optimized using the Box–Behnken response surface method, yielding optimal parameters: a catalyst addition of 0.97 wt%, esterification/polycondensation temperatures of 224 °C/216 °C, and a reaction time of 2.3 hours. Under these conditions, the copolymers exhibited an intrinsic viscosity of 0.57 dL g^{-1}. Structural characterization results (FTIR, NMR, XRD) confirmed the successful incorporation of EG into the polyester backbone without altering its crystalline structure. GPC measurements of PESG revealed a molecular weight of 2.2 × 10^4 g mol^{-1} and a dispersity index of 1.95. As the EG content increased, the T_g decreased to −18.8 °C, crystallinity declined, and segmental mobility improved. Notably, PESG demonstrated optimal hydrophilicity and biodegradability, with a 75% mass loss within 24 days under lipase treatment and a contact angle reduction to 53.6°. This study validates the feasibility of recycling electrolyte waste to synthesize degradable copolyesters, offering a novel pathway for the high-value utilization of electrolyte resources and the development of environmentally friendly materials.

Received 14th December 2025
Accepted 22nd January 2026

DOI: 10.1039/d5ra09672c

rsc.li/rsc-advances

Open Access Article. Published on 28 January 2026. Downloaded on 6/14/2026 2:35:37 PM.
This article is licensed under a Creative Commons Attribution-NonCommercial 3.0 Unported Licence.

1. Introduction

With the rapid development of new energy vehicles, energy storage systems, and portable electronic devices, the demand for lithium-ion batteries (LIBs) as core energy storage units continues to rise.[1] According to statistics, China's lithium battery production reached 940 GWh in 2023 and is projected to exceed 1100 GWh in 2024, with an annual growth rate surpassing 27%.[2,3] However, alongside the rapid expansion of production capacity, significant challenges related to waste battery recycling and environmental management have emerged. Over the next 5–10 years, a substantial influx of end-of-life batteries is expected as they reach the end of their service life. Due to their high chemical reactivity and potential toxicity, improper handling of the organic electrolyte components within these batteries poses serious risks of environmental pollution and safety hazards. Organic carbonates commonly found in electrolytes—such as ethylene carbonate (EC) and dimethyl carbonate (DMC)—exhibit high polarity, volatility, and reactivity. Notably, EC demonstrates strong thermal stability even at elevated temperatures, making it a valuable organic intermediate with significant potential for chemical conversion.[4–9] Therefore, achieving efficient separation and reuse of EC could not only mitigate its environmental impact but also provide essential raw material support for synthesizing downstream functional polymer materials.[10–18]

Polyethylene glycol succinate (PES), as a typical aliphatic biodegradable polyester,[10] exhibits excellent thermoplasticity, biodegradability, and processability. It has been widely applied

Shenyang University of Technology, Liaoyang 111003, China. E-mail: lyguo1981@163.com; albert_why@163.com

† These authors contributed to the work equally and should be regarded as co-first authors.

© 2026 The Author(s). Published by the Royal Society of Chemistry

Open Access Article. Published on 28 January 2026. Downloaded on 6/14/2026 2:35:37 PM. This article is licensed under a Creative Commons Attribution-NonCommercial 3.0 Unported Licence.

in fields such as packaging films, agricultural films, and biomedical materials. The primary synthesis methods involve melt polycondensation of ethylene oxide and/or ethylene glycol with succinic acid.[19–22] There are also isolated reports of PES being prepared *via* transesterification of ethylene carbonate and dimethyl succinate,[23,24] providing an important reference for the utilization of ethylene carbonate recovered from waste electrolytes in this study.

However, traditional PES materials face several challenges, including low mechanical strength, insufficient flexibility, and limited molecular weight, necessitating modification and optimization through molecular structure design.[25–29] Currently, common modification strategies include incorporating long-chain diols, aromatic monomers, or controlling segment composition and crystallization behavior through copolymerization. Nevertheless, these approaches often rely on petroleum-based raw materials, which can be costly and present limitations for green applications.[30–33]

For instance, Kondratowicz *et al.*[34] synthesized poly(ethylene succinate-*co*-terephthalate) (PES-*co*-PET) copolymers *via* melt polycondensation and investigated their chemical structure, thermal properties, and hydrolytic degradation behavior. Similarly, Terzopoulou *et al.*[35] synthesized fully bio-based copolyesters (PEFSu) using melt polycondensation. Their findings revealed that enzymatic degradation of the copolymer increased with higher succinic acid unit content, and when the succinic acid content exceeded 50 mol%, the degradation rate was significantly accelerated. Additionally, research groups led by Liu *et al.*[36] and Sun *et al.*[37] have made significant advancements in modifying biodegradable polyesters, providing a theoretical foundation for the research presented in this paper.

In light of this, based on the principles of green chemistry and circular economy, this study proposes a novel approach to synthesize basic polyester PES using EC recovered from spent lithium battery electrolytes as the raw material. The process involves coupling with biodegradable dicarboxylic acid ester DMSu to form the base polyester, followed by copolymerization modification with short-chain flexible diol EG as the third monomer to produce a series of copolyester PESG. This strategy aims to enhance material flexibility and biodegradability while achieving high-value utilization of organic solvents in spent electrolytes. Through systematic optimization of reaction parameters using Box–Behnken response surface methodology, combined with results from FTIR, NMR, TG curves, DCS curves, and XRD curves, the study explores the influence mechanism of the molar ratio of EC to EG (*i.e.*, EG addition amount) on the structural properties, thermal performance, crystallinity, water contact angle, and degradation behavior of the PESG series. These findings provide theoretical basis and data support for developing green, biodegradable, and high-performance polyester materials.

2. Materials and methods

2.1 Material and electrolyte recovery

The spent lithium-ion battery electrolyte used in the experiment was supplied by Suzhou Dingcheng New Energy Technology Co., Ltd, with main components including ethylene carbonate (EC), dimethyl carbonate (DMC), and lithium hexafluorophosphate ($LiPF_6$). To obtain high-purity EC, vacuum distillation was employed for separation and purification: initial distillation was performed at 150 °C and 0.09 MPa under atmospheric pressure, followed by further distillation under nitrogen protection in a rotary evaporator to recover EC. The product was analyzed by gas chromatography (GC) and Fourier transform infrared spectroscopy (FTIR), confirming a purity of 96.9% and a recovery rate of 86.5%. The obtained EC requires no further processing before use and can be directly incorporated into polyester synthesis reactions.

2.2 Synthesis methods for PES and PESG

PES was synthesized *via* melt polycondensation using recycled EC and DMSu as raw materials, with Bu_2SnO serving as the catalyst. The reaction was carried out in two stages: first, transesterification was performed under a nitrogen atmosphere at 200 °C for 4 hours; second, polymerization was conducted under reduced pressure at 215 °C for 2 hours. The resulting PES was precipitated in methanol and subsequently vacuum-dried at 60 °C for 24 hours to remove residual monomers. The experimental setup is illustrated in Fig. 1.

To enhance the flexibility and biodegradability of the material, EG was introduced as a third monomer to copolymerize with EC and DMSu, yielding a series of copolyesters (PESG). The EC : EG molar ratios were systematically adjusted to 10 : 0, 9 : 1, 8 : 2, 7 : 3, 6 : 4, and 5 : 5 (PES, $PESG_1$, $PESG_2$, $PESG_3$, $PESG_4$, $PESG_5$). The reaction was carried out in a 250 mL three-necked flask equipped with a mechanical stirrer, condenser, and vacuum system.

The one-pot process consisted of three sequential steps: deoxygenation: conducted under a nitrogen atmosphere at 60 °C to remove dissolved oxygen; esterification: performed at 210 °C until no further alcohol distillation was observed, indicating completion of the esterification reaction; polymerization: gradually heated to 215–220 °C for 2–3 hours under vacuum to facilitate polycondensation.

Upon completion of the reaction, the resulting polymer was precipitated in excess methanol, filtered, and subsequently vacuum-dried to remove residual solvents and unreacted monomers. The dried samples were then subjected to further characterization.

2.3 Optimize response surface design

To optimize the process conditions for PESG synthesis, a four-factor, three-level experimental design was implemented using Box–Behnken response surface methodology (RSM). The factors investigated included: (*A*) catalyst addition amount (0.8–1.2 wt%); (*B*) transesterification reaction temperature (210–230 °C); (*C*) polymerization reaction temperature (210–220 °C), and (*D*) reaction time (2.0–2.5 h).

A total of 27 experimental schemes were generated using Design-Expert software, with the intrinsic viscosity of the product serving as the response variable. Variance analysis was performed to evaluate the significance of each factor and their

© 2026 The Author(s). Published by the Royal Society of Chemistry

Open Access Article. Published on 28 January 2026. Downloaded on 6/14/2026 2:35:37 PM. This article is licensed under a Creative Commons Attribution-NonCommercial 3.0 Unported Licence.

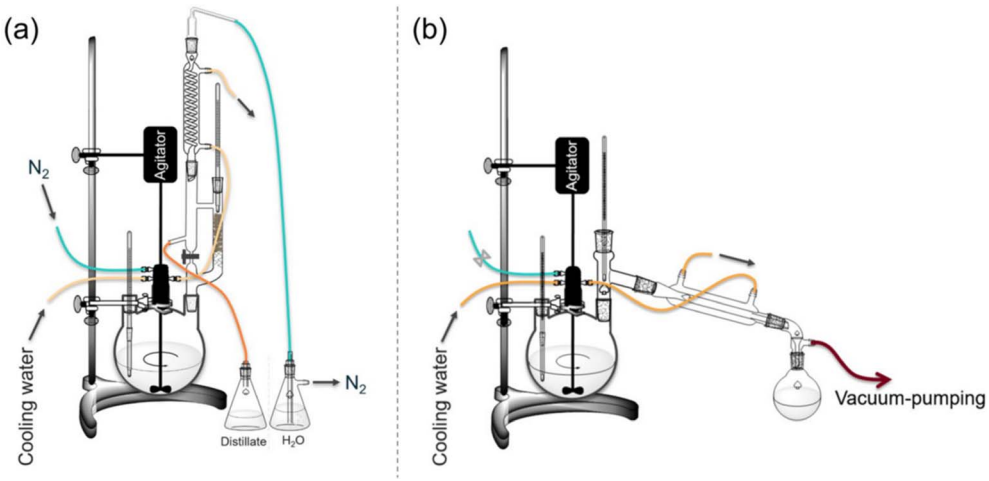

Fig. 1 Diagram of the reaction device for the synthesis of PES and its copolymers. (a) EC extraction device; (b) PES synthesis device.

interactions, ultimately identifying the optimal process combination. Repeated validation experiments were conducted to confirm the reliability of the optimized conditions.

The method for determining the intrinsic viscosity of the product is as follows: PES copolyester was quantitatively dissolved in chloroform to prepare a clear solution with a concentration of 1 g dL^{-1}. The solution was heated to 30 °C using a water bath, and the flow times of pure chloroform and the PES-chloroform solution were measured using a Ubbelohde viscometer with an inner diameter of 0.37 mm. Each liquid was tested three times, and the average flow time was calculated, ensuring the results were within the acceptable error range. The intrinsic viscosity was calculated using the following equation:

$$[\eta] = K \times M^{\alpha}$$

where $K = 2.4 \times 10^{-4}$ and $\alpha = 0.75$.

2.4 Performance characterization method

The structure of the polyester samples was characterized using Fourier transform infrared spectroscopy (FTIR, Bruker Vertex 70) and proton nuclear magnetic resonance spectroscopy (^{1}H-NMR, Bruker 400 MHz, $CDCl_3$) to confirm the successful incorporation of EG into the polymer main chain. The molecular weight and its distribution were determined by gel permeation chromatography (GPC, Agilent 1260), with chloroform as the mobile phase at a temperature of 35 °C.

Thermal properties were analyzed using thermogravimetric analysis (TGA, Shimadzu DTG-60) and differential scanning calorimetry (DSC, NETZSCH DSC 204F1). Thermal stability and T_g were measured under a nitrogen atmosphere at a heating rate of 10 °C min^{-1}. The crystal structure of the samples was determined using X-ray diffraction (XRD, Bruker D8 Advance) with Cu Kα radiation ($\lambda = 0.15418$ nm).

Hydrophilicity was assessed by measuring the water contact angle using a contact angle meter (Kruss DSA30).

2.4.1 Microbial degradation. *Aspergillus niger* (ATCC 16404) was selected as the biodegrading strain. *Aspergillus* spores were inoculated into potato dextrose agar (PDA) medium and cultured under constant temperature oscillation at 30 °C and 150 rpm for 72 hours to prepare a seed solution with a spore concentration of 1×10^6 CFU mL^{-1}.

Porcine pancreatic lipase (Sigma-Aldrich, L3126) was used as the enzymatic agent. A precise amount of 0.1 g lipase was dissolved in 100 mL of pre-cooled phosphate-buffered saline (PBS, pH 7.0) and magnetically stirred at 4 °C for 30 minutes. The mixture was then filtered through a 0.22 μm membrane for sterilization and used immediately.

2.4.2 Sample preparation and testing. PES copolyester was cast into films of dimensions 10 mm × 10 mm × 0.1 mm and vacuum-dried at 60 °C until reaching a constant weight, denoted as m_0. For testing, 1 mL of PDA medium containing either 0.1 mL of the *Aspergillus* spore solution or the prepared enzyme solution was added to separate wells of a 24-well plate. The samples were sealed and incubated under constant temperature oscillation at 37 °C and 120 rpm. Samples were collected and weighed every 3 days, and after 24 days, the samples were dried and weighed again to record the final mass as m_t. The remaining mass of the degraded PES copolyester was calculated using the formula:

$$\text{Remaining mass (\%)} = m_0/m_t \times 100\%.$$

3. Results and discussion

3.1 Synthesis process optimization and response surface analysis

To achieve the controllable synthesis of high molecular weight PESG and enhance reaction efficiency and product performance, this study systematically optimized four key parameters—catalyst dosage (A), ester exchange reaction temperature (B), polymerization temperature (C), and reaction time (D)—using Box–Behnken response surface methodology. Here, η denotes the product viscosity, with coefficients indicating the respective influence of each parameter on the response value. The experimental designs and results are presented in Table S1,

Open Access Article. Published on 28 January 2026. Downloaded on 6/14/2026 2:35:37 PM. This article is licensed under a Creative Commons Attribution-NonCommercial 3.0 Unported Licence.

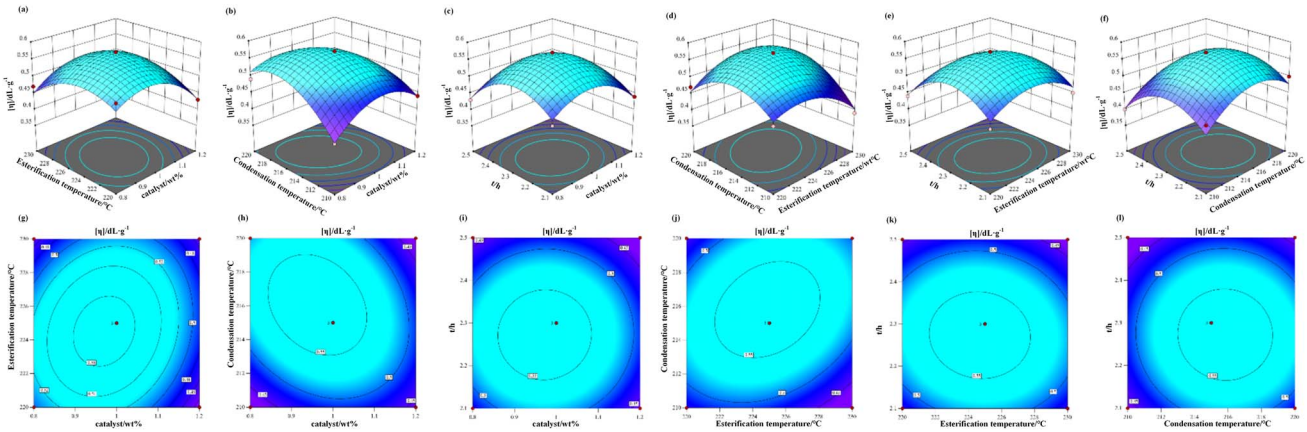

Fig. 2 (a–f) Contour lines between the RSM plot; (g–l) 3D response surface plot of each factor.

while the coded variable levels are detailed in Table S2. Statistical validation of the model was performed using analysis of variance (ANOVA).

As shown in Tables S1 and S2, the regression model demonstrates high significance (F-value: 10.83, $p < 0.0001$) and reliability. Factors A, C, D, AC, BC, A^2, B^2, C^2, and D^2 exhibit p-values < 0.05, indicating their significant effects on the characteristic viscosity of PES copolyester. In contrast, factors B, AB, AD, BD, and CD show p-values > 0.05, suggesting negligible influence. The correlation coefficient R^2 reaches 0.9266, with an adjusted R^2 of 0.8411 (difference: 0.0855 < 0.2), confirming the model's validity and its ability to explain most data variations. The quadratic regression model exhibits strong statistical significance. A linear relationship exists between the response variable Y (characteristic viscosity) and the influencing factors A, B, C, and D, making this model suitable for predicting the characteristic viscosity of PES copolyester.

By randomly selecting two factors (X-axis) from the four variables—catalyst dosage (A), esterification temperature (B), polycondensation temperature (C), and polycondensation time (D)—and plotting them against the characteristic viscosity (Y-axis), six response surface curves and corresponding contour lines were generated. These visual representations are presented in Fig. 2, providing insights into the interactions between the factors and their combined effects on the response variable.

As illustrated in the figures, using Fig. 2(b) and (h) as examples, the 3D response surface plots reveal that when the catalyst dosage is held constant, the characteristic viscosity of PES copolyester initially increases and subsequently decreases with rising polycondensation temperature. Conversely, when the polycondensation temperature is fixed, the characteristic viscosity exhibits a slight upward trend followed by a decline as the catalyst dosage increases, though the overall fluctuations remain relatively small. Notably, the steepness of the curve associated with polycondensation temperature is more pronounced than that of the catalyst dosage curve, indicating that polycondensation temperature exerts a more significant influence on the characteristic viscosity of PES copolyester compared to catalyst dosage.

In the contour plots, the ellipticity of the contour lines is not prominent, suggesting minimal interaction between the two factors—a conclusion consistent with the results obtained from software analysis. Based on the provided diagrams, the relative influence of the four factors on the characteristic viscosity of PES copolyester can be ranked as follows: polycondensation temperature (C) > polycondensation time (D) > catalyst dosage (A) > esterification temperature (B).

The single-factor response surface analysis demonstrated that both catalyst dosage and ester exchange temperature significantly influence product viscosity, with notable interaction effects. Within the catalyst dosage range of 0.95–1.05 wt%, increasing the ester exchange temperature promotes reaction progression. However, temperatures exceeding 225 °C may induce side reactions, potentially leading to molecular chain degradation.

Polymerization temperature exhibits a positive correlation with the degree of polymerization, with the optimal range identified as 214–218 °C. Regarding reaction time, viscosity increases markedly during the first 2.2–2.4 hours, after which it

Table 1 Best process conditions and verification results

Catalyst dosage (A) (wt%)	Esterification temperature (B) (°C)	Condensation temperature (C) (°C)	Condensation time (D) (h)	Intrinsic viscosity prediction [η] (dL g^{-1})	Actual viscosity [η] (dL g^{-1})	Intrinsic viscosity average
0.973	224.161	216.282	2.282	0.57	0.56 0.56 0.57	0.56

© 2026 The Author(s). Published by the Royal Society of Chemistry

Open Access Article. Published on 28 January 2026. Downloaded on 6/14/2026 2:35:37 PM. This article is licensed under a Creative Commons Attribution-NonCommercial 3.0 Unported Licence.

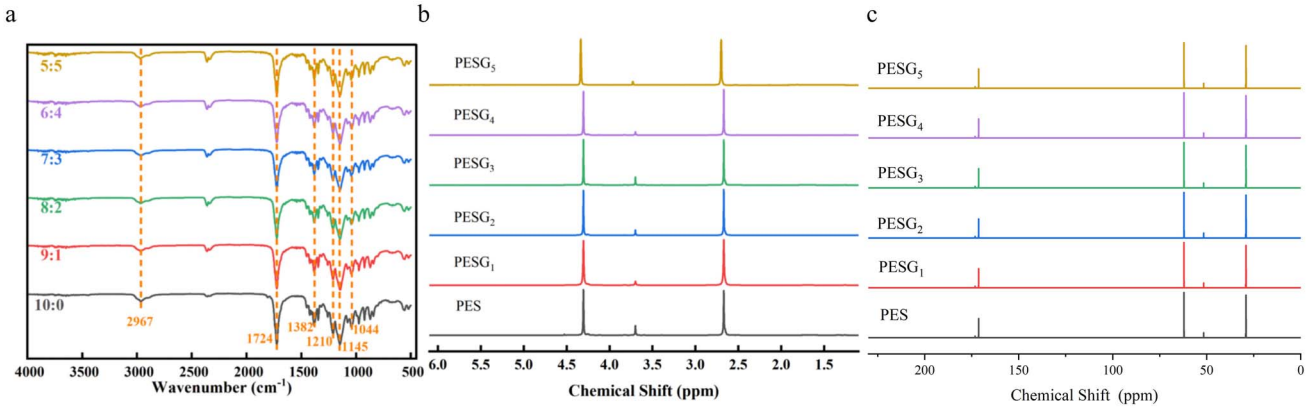

Fig. 3 Molecular structure analysis of PES and PESG$_x$. (a) Infrared spectra of PES and PESG$_x$; (b) ^{1}H-NMR spectrum of PES and PESG$_x$; (c) ^{13}C-NMR spectrum of PES and PESG$_x$.

plateaus beyond 2.5 hours. This plateau is likely attributed to excessive viscosity, which hinders material flow and reduces mass transfer efficiency.

The optimized process conditions, along with their validation results, are summarized in Table 1.

The optimal process parameters were determined through response surface optimization analysis as follows: a catalyst dosage of 0.97 wt%, an ester exchange temperature of 224 °C, a polymerization temperature of 216 °C, and a reaction time of 2.3 hours. Under these conditions, the synthesized PESG samples achieved a viscosity of 0.57 dL g^{-1}, representing a 35% improvement compared to the initial conditions. This result effectively validates the accuracy and reliability of the model predictions.

3.2 Molecular structure and chemical composition analysis

To verify the copolymerization reaction and the successful incorporation of EG monomer, FTIR and NMR were employed to characterize the structures of the synthesized PES and PESG copolymers. The characterization results are shown in Fig. 3.

The FTIR spectra of all samples revealed C–H stretching vibrations at 2945 cm^{-1} and 2872 cm^{-1}, along with a prominent C=O stretching absorption peak at 1725 cm^{-1}, confirming the successful formation of ester groups. Additionally, characteristic C–O–C absorption peaks were observed near 1158 cm^{-1} and 1045 cm^{-1}, indicating the presence of ester linkages in the polyester backbone. As the EG content increased, the absorption peak at 1045 cm^{-1} showed slight intensification, suggesting a higher proportion of C–O bond structures and corroborating the participation of EG monomer in the copolymerization process.

The NMR spectral results further supported these findings. In the proton NMR spectrum, the characteristic peak at δ = 4.35 ppm, along with the peak at δ = 62.06 ppm in the carbon NMR spectrum, was attributed to the –CH_2– signal originating from EC/EG units. Meanwhile, a newly observed peak near δ = 2.65 ppm in the proton spectrum and a peak at δ = 29.20 ppm in the carbon spectrum were assigned to the –CH_2– signal from DMSu. Furthermore, the peak at δ = 171.30 ppm in the carbon spectrum corresponded to the carbonyl carbon, confirming the complete triad copolymerization of the monomers. Through integral ratio calculations, the monomer composition ratios in samples with varying EG contents were found to align closely with the designed feedstock ratios, demonstrating excellent compositional control during the copolymerization process.

The analysis of the above characterization results confirms that this study successfully achieved the ternary copolymerization of EC, DMSu, and EG *via* a one-step method. The resulting PESG copolyester exhibits a clear structure and controllable composition, providing a solid foundation for tailoring its properties and performance.

3.3 Molecular weight and distribution analysis

GPC was employed to determine the molecular weight and distribution of the synthesized PES and PESG samples with varying EG copolymer ratios, and t_o analyze their chain segment configurations and polymerization behaviors. The results are presented in Table 2.

The test results reveal that the number-average molecular weight (M_n) of pure PES samples is 1.6 × 10^4 g mol^{-1}, with a dispersion coefficient ($Đ$) of 2.10, indicating a relatively broad molecular weight distribution. When the EG content is moderately increased, the polymerization reaction activity significantly improves. For instance, in PESG2 samples, M_n increases to 2.2 × 10^4 g mol^{-1}, while $Đ$ decreases to 1.95, reflecting enhanced uniformity in chain growth during the

Table 2 Characteristics of PES and PESG$_x$, including intrinsic viscosity and average molecular weight

Sample number	$[\eta]$ (dL g^{-1})	M_η/10^4 g mol^{-1}
PES	0.42	2.00
PESG$_1$	0.51	2.54
PESG$_2$	0.56	2.88
PESG$_3$	0.54	2.79
PESG$_4$	0.50	2.50
PESG$_5$	0.48	2.36

© 2026 The Author(s). Published by the Royal Society of Chemistry

Open Access Article. Published on 28 January 2026. Downloaded on 6/14/2026 2:35:37 PM. This article is licensed under a Creative Commons Attribution-NonCommercial 3.0 Unported Licence.

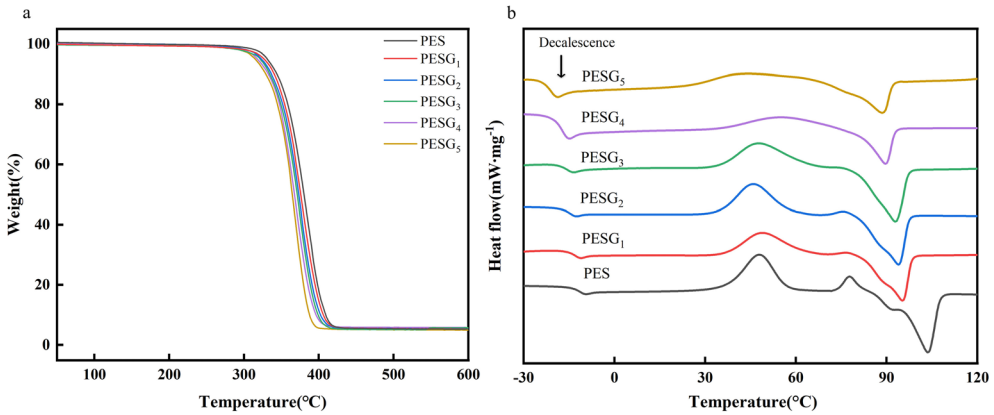

Fig. 4 Thermal performance analysis of PES and PESG$_x$. (a) DSC curves for PES and PESG$_x$; (b) thermogravimetric curve plots of PES and PESG$_x$.

copolymerization process. This improvement can be attributed to the shorter molecular chains of EG, which enhance the fluidity of the reaction mixture and increase the reaction migration rate, thereby improving the efficiency of ester exchange and condensation polymerization.

However, when the EG feeding ratio is increased to 5 : 5, M_n decreases to 1.7 × 10^4 g mol^{-1}, and $Đ$ slightly rises to 2.03. Analysis suggests that higher EG content elevates the hydroxyl functionality within the system, potentially triggering excessive branching or chain termination reactions that inhibit further molecular weight growth. Consequently, while moderate EG introduction enhances the degree of polymerization and improves reaction control, excessive EG content impedes main chain extension. These findings underscore the importance of carefully regulating EG content in copolymer design to optimize molecular weight and structural control.

3.4 Thermal performance analysis

The thermal properties of PES and PESG copolymers were evaluated using DSC and TGA to investigate the effects of EG incorporation on their thermal stability and phase transition behavior. The DSC and TGA curves are shown in Fig. 4.

DSC test results indicate that the glass transition temperature (T_g) of pure PES samples is −9.5 °C, with a melting temperature (T_m) of 96.8 °C. As EG content increases, the T_g of PESG series samples gradually decreases, with PESG3 reaching -18.8 °C and T_m slightly dropping to 93.1 °C. This phenomenon is attributed to EG introducing flexible –CH_2CH_2– segments, which enhance molecular chain flexibility, weaken intermolecular forces, and reduce the energy barrier for polymer chain movement. Concurrently, the broadening and weakening of the melting peak suggest reduced crystallinity and a trend toward disordered crystalline structures.

TGA analysis further validated the variation trend of the material's thermal stability. The 5% mass loss temperature ($T_{d,5\%}$) of PES samples was 315 °C, which slightly decreased after EG copolymerization, as evidenced by PESG$_3$'s $T_{d,5\%}$ of 305 °C. This may be attributed to the relatively weak thermal stability of C–O bonds in the EG structure, leading to a lower initial decomposition temperature. Nevertheless, the primary thermal decomposition range of all PESG samples remained concentrated between 290 and 410 °C, demonstrating overall good thermal stability that meets the thermal performance requirements for most biodegradable applications.

In conclusion, the appropriate introduction of EG significantly improves the flexibility and chain mobility of polyester, reduces the glass transition temperature (T_g), and facilitates processing and application in low-temperature environments. It also maintains high thermal stability, achieving an optimal balance between thermal and mechanical properties.

3.5 Crystal structure and crystallization behavior analysis

To investigate the effect of EG copolymerization on the crystal structure and crystallization behavior of PES, XRD was employed to characterize the crystal structures of the samples. The characterization results are shown in Fig. 5.

The PES samples displayed distinct diffraction peaks at 2θ = 21.2°, 23.5°, and 25.9°, corresponding to the characteristic (110), (020), and (021) crystal planes of the α crystalline form.

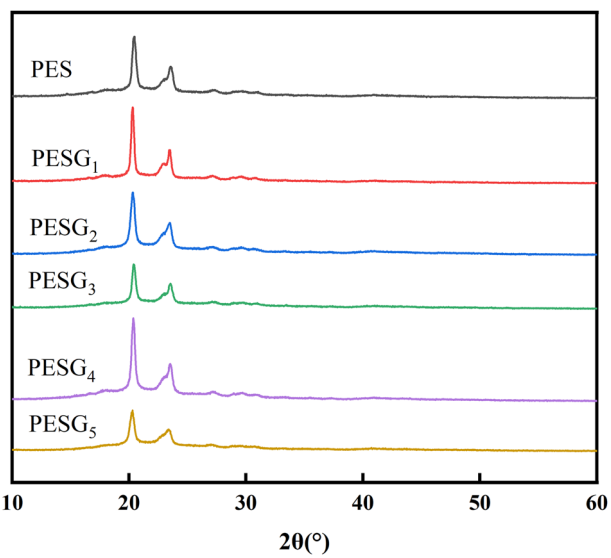

Fig. 5 X-ray diffraction spectra of PES and PESG$_x$.

© 2026 The Author(s). Published by the Royal Society of Chemistry

Open Access Article. Published on 28 January 2026. Downloaded on 6/14/2026 2:35:37 PM. This article is licensed under a Creative Commons Attribution-NonCommercial 3.0 Unported Licence.

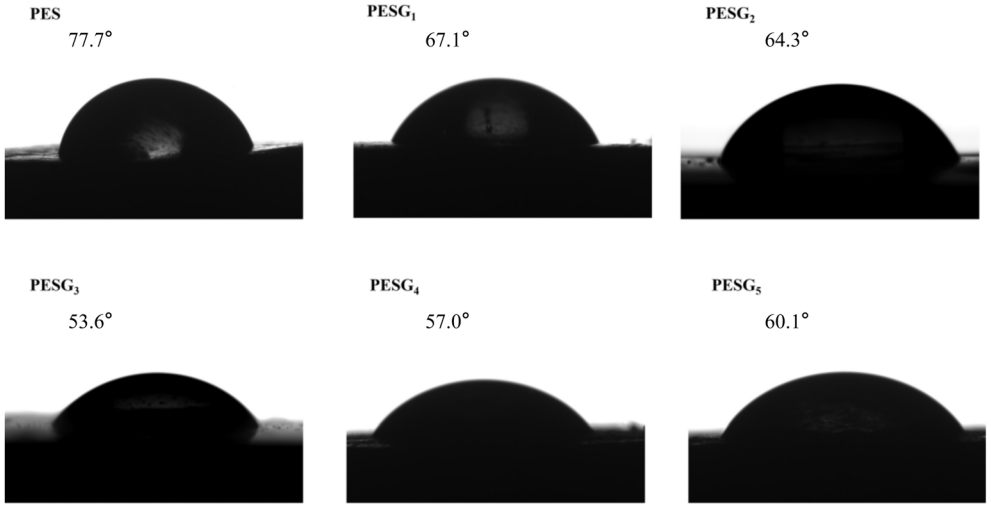

Fig. 6 Water contact angle test chart of PES and $PESG_x$.

These peaks indicate a high degree of crystallinity and a well-defined crystal structure. However, as the EG content increased, the intensity of these diffraction peaks gradually diminished, while their half-peak widths broadened. This suggests a reduction in grain size, decreased crystallinity, and an increased proportion of amorphous regions, indicative of a partially disordered structure within the material.

Although EG copolymerization impacts crystallinity, it does not alter the type of crystal structure in PES. All samples consistently exhibit the same diffraction peak positions, retaining the α crystalline structure. This indicates that EG primarily disrupts the crystallization process at the chain segment level without inducing new structural transformations. While the reduction in crystallinity enhances material flexibility and transparency, it may also result in a decrease in the heat deformation temperature. Therefore, in practical applications, the EG addition ratio should be carefully optimized based on crystallinity control requirements to achieve a balance between mechanical properties and processability.

3.6 Surface hydrophilicity and biodegradability

Biodegradable materials must meet stringent environmental adaptability and degradation performance requirements in practical applications. This study systematically evaluated the hydrophilicity and biodegradability of PESG copolymers through contact angle measurements and enzymatic degradation experiments. The hydrophilicity characterization results are shown in Fig. 6.

The contact angle measurements demonstrated that the static water contact angle of pure PES samples was 76.2°. As the ethylene glycol (EG) copolymerization ratio increased, the contact angle progressively decreased, reaching 53.6° for $PESG_3$ samples. This trend indicates a significant improvement in the material's surface hydrophilicity, primarily attributed to the incorporation of EG segments. These segments increase the polarity of the molecular chains and enhance the surface's affinity for water molecules. The improved hydrophilicity facilitates better interaction between the degradation medium and the material, thereby promoting subsequent biodegradation processes.

The mass data of the residual samples from the biodegradation and enzymatic degradation experiments are shown in Fig. 7.

The samples were incubated in lipase-containing PBS buffer or spore seed solution for 24 days at 37 °C. As shown in Fig. 7, the mass loss rate in the enzymatic group on day 24 ranged from 65.94% ± 3.38% to 75.31% ± 3.38%, while that in the biodegradation group was 61.03% ± 3.15% to 71.26% ± 3.15%. A one-way ANOVA was performed on the experimental data to verify the overall difference in mass loss rates between the two groups. The results demonstrated a highly significant difference in mass loss rates between the enzymatic and biodegradation groups ($P < 0.001$), with the enzymatic group exhibiting

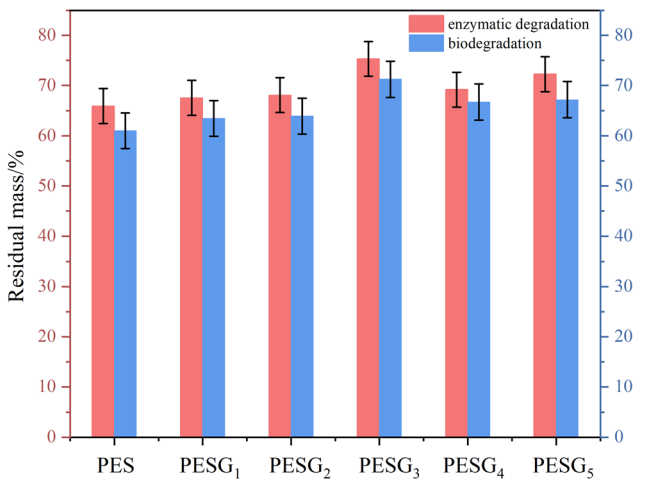

Fig. 7 Residual sample mass percentage in biodegradation and enzymatic degradation experiments.

Open Access Article. Published on 28 January 2026. Downloaded on 6/14/2026 2:35:37 PM. This article is licensed under a Creative Commons Attribution-NonCommercial 3.0 Unported Licence.

approximately 34% higher mass loss rates compared to the biodegradation group.

Under these conditions, pure PES samples exhibited only about 35% mass loss, whereas $PESG_3$ samples showed a mass loss rate as high as 75%, significantly enhancing degradation efficiency. This phenomenon is attributed to the increased flexibility of EG segments and the higher proportion of amorphous regions, which facilitate enzyme recognition and hydrolysis of polymer chains. Additionally, the lower crystallinity accelerates water molecule diffusion within the material, further promoting the exposure of enzyme action sites.

The results show that EG copolymerization not only improves the surface wettability of the material, but also significantly enhances its degradation rate under physiological conditions, providing strong support for the development of environmentally friendly degradable polyester materials.

The samples were incubated in lipase-containing PBS buffer or spore seed solution for 24 days at 37 °C. As shown in Fig. 7, the mass loss rate in the enzymatic group on day 24 ranged from 65.94% ± 3.38% to 75.31% ± 3.38%, while that in the biodegradation group ranged from 61.03% ± 3.15% to 71.26% ± 3.15%. A one-way ANOVA was performed on the experimental data to verify the overall difference in mass loss rates between the two groups. The results demonstrated a highly significant difference in mass loss rates between the enzymatic and biodegradation groups ($P < 0.001$), with the enzymatic group exhibiting approximately 34% higher mass loss rates compared to the biodegradation group.

Under these conditions, pure PES samples exhibited only about 35% mass loss, whereas $PESG_3$ samples showed a mass loss rate as high as 75%, significantly enhancing degradation efficiency. This phenomenon can be attributed to the increased flexibility of EG segments and the higher proportion of amorphous regions, which facilitate enzyme recognition and hydrolysis of polymer chains. Additionally, the lower crystallinity accelerates water molecule diffusion within the material, further promoting the exposure of enzyme action sites.

These results indicate that EG copolymerization not only improves the surface wettability of the material but also significantly enhances its degradation rate under physiological conditions. This provides strong support for the development of environmentally friendly degradable polyester materials.

4. Conclusion

This study, rooted in the concept of high-value resource utilization, introduces a novel approach to synthesizing degradable polyester material PESG using EC recovered from spent lithium battery electrolytes as a raw material. The synthesis involves the polycondensation of EC with DMSu to form the base polyester PES, followed by the incorporation of EG as a third monomer for copolymer modification. We systematically investigated the effects of EG content on the structure and properties of PESG. To optimize the synthesis process, the Box–Behnken response surface methodology was employed, yielding the optimal parameter combination: catalyst concentration of 0.97 wt%, ester exchange/polycondensation temperatures of 224 °C/216 °C, and reaction time of 2.3 hours. Under these conditions, the synthesized PESG copolymer achieved an intrinsic viscosity of 0.57 dL g^{-1}.

Structural characterization confirmed the successful incorporation of EG into the polymer main chain without altering the crystal morphology. GPC analysis revealed that an appropriate EG content increased molecular weight and improved molecular weight distribution. Thermal analysis demonstrated that the introduction of EG reduced the T_g, enhancing material flexibility while maintaining high thermal stability. XRD results indicated that EG decreased crystallinity and increased chain segment disorder, contributing to a more amorphous structure. Contact angle measurements and enzymatic degradation experiments further confirmed enhanced hydrophilicity and significantly improved biodegradability of the material.

In conclusion, this study proposes a green and biodegradable copolyester material development strategy that balances environmental friendliness with tunable performance. By utilizing organic solvents recovered from waste electrolytes, this approach not only addresses environmental concerns but also expands the application potential of PES-based copolymers in sustainable materials. This work provides a novel pathway for the resource utilization of waste materials and contributes to the advancement of eco-friendly polymer technologies.

Conflicts of interest

No conflicts of interest needs to be declared.

Data availability

The authors confirm that the data supporting the findings of this study are available within the article or its supplementary information (SI). Supplementary information: comprehensive experimental protocols for ethylene carbonate recovery and PESG synthesis, as well as full characterization spectra (^{1}H NMR, ^{13}C NMR, FT-IR, GPC, DSC/TGA) with peak assignments. Additional figures and tables illustrate the effects of reaction parameters and provide reproducibility data, cross-referenced to relevant sections in the main text. All SI adheres to *RSC Advances* guidelines, with consistent nomenclature and machine-readable formats for accessibility. See DOI: https://doi.org/10.1039/d5ra09672c.

References

1 J.-M. Tarascon and M. Armand, Issues and Challenges Facing Rechargeable Lithium Batteries, *Nature*, 2001, **414**(6861), 359–367, DOI: 10.1038/35104644.

2 M. D. Tikekar, S. Choudhury, Z. Tu and L. A. Archer, Design Principles for Electrolytes and Interfaces for Stable Lithium-Metal Batteries, *Nat. Energy*, 2016, **1**(9), 16114, DOI: 10.1038/nenergy.2016.114.

3 Y. Liu, C. Zhao, J. Du, X. Zhang, A. Chen and Q. Zhang, Research Progresses of Liquid Electrolytes in Lithium-Ion Batteries, *Small*, 2023, **19**(8), 2205315, DOI: 10.1002/smll.202205315.

© 2026 The Author(s). Published by the Royal Society of Chemistry

Open Access Article. Published on 28 January 2026. Downloaded on 6/14/2026 2:35:37 PM. This article is licensed under a Creative Commons Attribution-NonCommercial 3.0 Unported Licence.

4 Y. Liu, M. Su, Z. Gu, K. Zhang, X. Wang, M. Du, J. Guo and X. Wu, Advanced Lithium Primary Batteries: Key Materials, Research Progresses and Challenges, *Chem. Rec.*, 2022, **22**(10), e202200081, DOI: 10.1002/tcr.202200081.

5 A. Mistry, V. Srinivasan and H. Steinrück, Characterizing Ion Transport in Electrolytes via Concentration and Velocity Profiles, *Adv. Energy Mater.*, 2023, **13**(9), 2203690, DOI: 10.1002/aenm.202203690.

6 S.-Y. Sun, X.-Q. Zhang, Y.-N. Wang, J.-L. Li, Z. Zheng and J.-Q. Huang, Understanding the Transport Mechanism of Lithium Ions in Solid-Electrolyte Interphase in Lithium Metal Batteries with Liquid Electrolytes, *Mater. Today*, 2024, **77**, 39–65, DOI: 10.1016/j.mattod.2024.06.001.

7 J.-C. Ye, Y.-W. Lai, X.-H. Huang, Z.-X. Chang, Y.-H. Chung and C.-M. Shu, Development of the Electrolyte in Lithium-Ion Battery: A Concise Review on Its Thermal Hazards, *J. Therm. Anal. Calorim.*, 2024, **149**(19), 11293–11312, DOI: 10.1007/s10973-024-13598-3.

8 S. Kainat, J. Anwer, A. Hamid, N. Gull and S. M. Khan, Electrolytes in Lithium-Ion Batteries: Advancements in the Era of Twenties (2020's), *Mater. Chem. Phys.*, 2024, **313**, 128796, DOI: 10.1016/j.matchemphys.2023.128796.

9 C.-C. Wu, T.-C. Chan and S.-H. Chung, Progress on Critical Cell Fabrication Parameters and Designs for Advanced Lithium–Sulfur Batteries, *Chem. Commun.*, 2024, **60**(79), 11017–11033, DOI: 10.1039/D4CC03085K.

10 H. Wan, J. Xu and C. Wang, Designing Electrolytes and Interphases for High-Energy Lithium Batteries, *Nat. Rev. Chem.*, 2023, **8**(1), 30–44, DOI: 10.1038/s41570-023-00557-z.

11 W. Li, Z. He, Y. Jie, F. Huang, Y. Chen, Y. Wang, W. Zhang, X. Zhu, R. Cao and S. Jiao, Understanding and Design of Cathode–Electrolyte Interphase in High-Voltage Lithium–Metal Batteries, *Adv. Funct. Mater.*, 2024, **34**(45), 2406770, DOI: 10.1002/adfm.202406770.

12 K. Xu, Li-Ion Battery Electrolytes, *Nat. Energy*, 2021, **6**(7), 763, DOI: 10.1038/s41560-021-00841-6.

13 Q. Wang, L. Jiang, Y. Yu and J. Sun, Progress of Enhancing the Safety of Lithium Ion Battery from the Electrolyte Aspect, *Nano Energy*, 2019, **55**, 93–114, DOI: 10.1016/j.nanoen.2018.10.035.

14 J.-K. Kim, A. Matic, J.-H. Ahn and P. Jacobsson, An Imidazolium Based Ionic Liquid Electrolyte for Lithium Batteries, *J. Power Sources*, 2010, **195**(22), 7639–7643, DOI: 10.1016/j.jpowsour.2010.06.005.

15 T. Sugimoto, Y. Atsumi, M. Kikuta, E. Ishiko, M. Kono and M. Ishikawa, Ionic Liquid Electrolyte Systems Based on Bis(Fluorosulfonyl)Imide for Lithium-Ion Batteries, *J. Power Sources*, 2009, **189**(1), 802–805, DOI: 10.1016/j.jpowsour.2008.07.053.

16 Y. Lan, L. Tan, N. Wu, J. Wen, W. Yao, Y. Tang and H.-M. Cheng, Current Status and Outlook of Recycling Spent Lithium-Ion Batteries, *J. Energy Storage*, 2025, **110**, 115374, DOI: 10.1016/j.est.2025.115374.

17 X. Li, H. Wang, W. Chang, X. Li, L. Deng and L. Guo, Progress in the Synthesis of Polyurethane Elastomers, *Russ. J. Appl. Chem.*, 2024, **97**(10), 778–789, DOI: 10.1134/S1070427225600531.

18 X. Li, H. Wang, L. Guo, X. Li, X. Li and L. Fan, Circular High-Value Utilization of Low-Boiling Components from Waste Lithium-Ion Battery Electrolytes: Diamino Carbamate-Mediated Synthesis of Sustainable Non-Isocyanate Polyurethanes, *Energy Fuels*, 2026, **40**(2), 1444–1453, DOI: 10.1021/acs.energyfuels.5c05262.

19 L. Miao, Z. Qiu, W. Yang and T. Ikehara, Fully Biodegradable Poly(3-Hydroxybutyrate-Co-Hydroxyvalerate)/Poly(Ethylene Succinate) Blends: Phase Behavior, Crystallization and Mechanical Properties, *React. Funct. Polym.*, 2008, **68**(2), 446–457, DOI: 10.1016/j.reactfunctpolym.2007.11.001.

20 F. Wu, C.-L. Huang, J.-B. Zeng, S.-L. Li and Y.-Z. Wang, Composition Dependence of Physical Properties of Biodegradable Poly(Ethylene Succinate) Urethane Ionenes, *RSC Adv.*, 2014, **4**(97), 54175–54186, DOI: 10.1039/C4RA05484A.

21 C. Liu, Biodegradable Poly(Ethylene Succinate-Co-Ethylene Oxalate-Co-Diethylene Glycol Succinate): Effects of a Small Amount of Ethylene Oxalate Content on the Properties of Poly(Ethylene Succinate), *Polymer*, 2021, **45**(2), 294–302, DOI: 10.7317/pk.2021.45.2.294.

22 J. C. Morales-Huerta, A. M. De Ilarduya and S. Muñoz-Guerra, A Green Strategy for the Synthesis of Poly(Ethylene Succinate) and Its Copolyesters via Enzymatic Ring Opening Polymerization, *Eur. Polym. J.*, 2017, **95**, 514–519, DOI: 10.1016/j.eurpolymj.2017.08.043.

23 X. Zhao, L. Guo, T. Xu, H. Wang, R. Zheng and Z. Jiang, Preparation of Biacidic Tin-Based Ionic Liquid Catalysts and Their Application in Catalyzing Coupling Reaction between Ethylene Carbonate and Dimethyl Succinate to Synthesize Poly(Ethylene Succinate), *New J. Chem.*, 2022, **46**(33), 15901–15910, DOI: 10.1039/D2NJ03225B.

24 X. Zhao, L. Guo, T. Xu, R. Zheng and H. Wang, Preparation of Keggin-Type Monosubstituted Polyoxometalate Ionic Liquid Catalysts and Their Application in Catalyzing the Coupling Reaction of Ethylene Carbonate and Dimethyl Succinate to Synthesize Poly(Ethylene Succinate), *New J. Chem.*, 2022, **46**(42), 20092–20101, DOI: 10.1039/D2NJ03094B.

25 Q.-Y. Zhu, Y.-S. He, J.-B. Zeng, Q. Huang and Y.-Z. Wang, Synthesis and Characterization of a Novel Multiblock Copolyester Containing Poly(Ethylene Succinate) and Poly(Butylene Succinate), *Mater. Chem. Phys.*, 2011, **130**(3), 943–949, DOI: 10.1016/j.matchemphys.2011.08.012.

26 G. Seretoudi, D. Bikiaris and C. Panayiotou, Synthesis, Characterization and Biodegradability of Poly(Ethylene Succinate)/Poly(ε-Caprolactone) Block Copolymers, *Polymer*, 2002, **43**(20), 5405–5415, DOI: 10.1016/S0032-3861(02)00433-0.

27 M. M. Abdelghafour, Á. Orbán, Á. Deák, Ł. Lamch, É. Frank, R. Nagy, A. Ádám, P. Sipos, E. Farkas, F. Bari and L. Janovák, The Effect of Molecular Weight on the Solubility Properties of Biocompatible Poly(Ethylene Succinate) Polyester, *Polymers*, 2021, **13**(16), 2725, DOI: 10.3390/polym13162725.

28 J. Li, Z. Jiang and Z. Qiu, Isothermal Melt Crystallization Kinetics Study of Cellulose Nanocrystals Nucleated Biodegradable Poly(Ethylene Succinate), *Polymer*, 2021, **227**, 123869, DOI: 10.1016/j.polymer.2021.123869.

Open Access Article. Published on 28 January 2026. Downloaded on 6/14/2026 2:35:37 PM. This article is licensed under a Creative Commons Attribution-NonCommercial 3.0 Unported Licence.

29 K.-J. Zhang and Z.-B. Qiu, Miscibility and Crystallization Behavior of Novel Branched Poly(Ethylene Succinate)/Poly(Vinyl Phenol) Blends, *Chin. J. Polym. Sci.*, 2019, **37**(11), 1169–1175, DOI: 10.1007/s10118-019-2269-1.

30 G. Z. Papageorgiou and D. N. Bikiaris, Synthesis and Properties of Novel Biodegradable/Biocompatible Poly [Propylene-Co-(Ethylene Succinate)] Random Copolyesters, *Macromol. Chem. Phys.*, 2009, **210**(17), 1408–1421, DOI: 10.1002/macp.200900132.

31 S. Pan, Z. Jiang and Z. Qiu, Significantly Enhanced Crystallization of Poly(Ethylene Succinate-Co-1,2-Propylene Succinate) by Cellulose Nanocrystals as an Efficient Nucleating Agent, *Polymers*, 2022, **14**(2), 224, DOI: 10.3390/polym14020224.

32 G. Z. Papageorgiou, Z. Terzopoulou, V. Tsanaktsis, D. S. Achilias, K. Triantafyllidis, E. K. Diamanti, D. Gournis and D. N. Bikiaris, Effect of Graphene Oxide and Its Modification on the Microstructure, Thermal Properties and Enzymatic Hydrolysis of Poly(Ethylene Succinate) Nanocomposites, *Thermochim. Acta*, 2015, **614**, 116–128, DOI: 10.1016/j.tca.2015.06.016.

33 Y.-S. He, J.-B. Zeng, S.-L. Li and Y.-Z. Wang, Crystallization Behavior of Partially Miscible Biodegradable Poly(Butylene Succinate)/Poly(Ethylene Succinate) Blends, *Thermochim. Acta*, 2012, **529**, 80–86, DOI: 10.1016/j.tca.2011.11.031.

34 F. Ł. Kondratowicz and R. Ukielski, Synthesis and Hydrolytic Degradation of Poly(Ethylene Succinate) and Poly(Ethylene Terephthalate) Copolymers, *Polym. Degrad. Stab.*, 2009, **94**(3), 375–382, DOI: 10.1016/j.polymdegradstab.2008.12.001.

35 Z. Terzopoulou, V. Tsanaktsis, D. N. Bikiaris, S. Exarhopoulos, D. G. Papageorgiou and G. Z. Papageorgiou, Biobased Poly(Ethylene Furanoate-Co-Ethylene Succinate) Copolyesters: Solid State Structure, Melting Point Depression and Biodegradability, *RSC Adv.*, 2016, **6**(87), 84003–84015, DOI: 10.1039/C6RA15994J.

36 C. Liu, J.-B. Zeng, S.-L. Li, Y.-S. He and Y.-Z. Wang, Improvement of Biocompatibility and Biodegradability of Poly(Ethylene Succinate) by Incorporation of Poly(Ethylene Glycol) Segments, *Polymer*, 2012, **53**(2), 481–489, DOI: 10.1016/j.polymer.2011.12.003.

37 Z. Sun, M. Chen, G. Xie, Z. Jiang and Z. Qiu, Synthesis and Properties of Biodegradable Poly(Ethylene Succinate) Containing Two Adjacent Side Methyl Groups, *Polymer*, 2023, **283**, 126300, DOI: 10.1016/j.polymer.2023.126300.

© 2026 The Author(s). Published by the Royal Society of Chemistry